

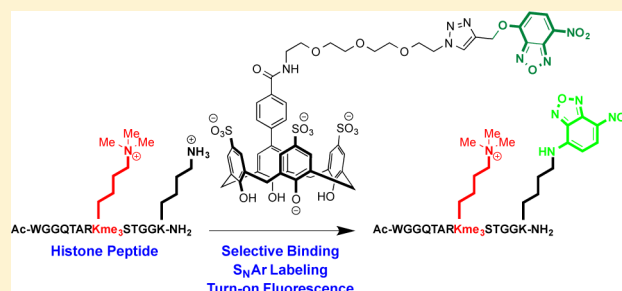
# Supramolecular Affinity Labeling of Histone Peptides Containing Trimethyllysine and Its Application to Histone Deacetylase Assays

Isaiah N. Gober and Marcey L. Waters\*

Department of Chemistry, CB 3290, UNC Chapel Hill, Chapel Hill, North Carolina 27599, United States

**S** Supporting Information

**ABSTRACT:** Lysine methylation is an important histone post-translational modification (PTM) for manipulating chromatin structure and regulating gene expression, and its dysregulation is associated with various diseases including many cancers. While characterization of Lys methylation has seen improvements over the past decade due to advances in proteomic mass spectrometry and methods involving antibodies, chemical methods for selective detection of proteins containing PTMs are still lacking. Here, we detail the development of a unique labeling method wherein a synthetic receptor probe for trimethyl lysine (Kme3), CX4-ONBD, is used to direct selective fluorescent labeling of Kme3 histone peptides. This supramolecular approach reverses the paradigm of ligand-directed affinity labeling by making the receptor the synthetic component and the ligand the component to be labeled. We show that the probe mediates a strong turn-on fluorescence response in the presence of a Kme3 histone peptide and shows >5-fold selectivity in covalent labeling over an unmethylated lysine peptide. We also demonstrate the utility of the probe through the design of a turn-on fluorescence assay for histone deacetylase (HDAC) activity and for inhibitor screening and IC<sub>50</sub> determination. Our synthetic receptor-mediated affinity labeling approach broadens the scope of PTM detection by chemical means and may facilitate the development of more versatile in vitro enzymatic assays.



## INTRODUCTION

Methylation of Lys and Arg in histone proteins is involved in many vital biological processes that regulate the dynamic structure of chromatin and alter the interactions of DNA with protein complexes. Accordingly, there is great interest in mapping out the epigenetic role of these post-translational modifications (PTMs) in development and disease.<sup>1–3</sup> Two of the most established methods to detect post-translational modifications of proteins include antibodies and mass spectrometry-based proteomics. While these methods are staples of PTM research, both face challenges and limitations. Antibodies often exhibit high sequence specificity, which complicates the detection of unknown PTMs.<sup>4,5</sup> Additionally, some antibodies suffer from irreproducibility from batch to batch and have been shown to have cross-reactivity with off-target antigens.<sup>6</sup> MS-based proteomics has been used to explore a number of PTMs including methylation of lysine and arginine,<sup>7–10</sup> acetylation of lysine,<sup>11,12</sup> and phosphorylation of serine and threonine.<sup>13</sup> However, MS analysis is expensive and time-consuming and can be complicated by analytical challenges including low natural abundance of PTMs, the presence of complex mixtures, and difficulties in analyzing large ionized proteins.<sup>14</sup>

Innovative tools for detecting PTMs would augment existing detection methods and expand the chemical tool kit available for epigenetics research. Specifically, approaches for site-selective covalent labeling of proteins or peptides containing

PTMs represent an emerging technology<sup>15,16</sup> that has great potential to further our understanding of how these modifications regulate gene expression and how the PTMs themselves are regulated. For example, direct covalent modification of citrulline has been developed to characterize citrullination.<sup>15</sup> Since trimethyllysine cannot be directly covalently labeled, indirect methods are needed. A popular approach has been to engineer methyltransferase enzymes to accept unnatural SAM analogues in order to transfer alkynes<sup>17</sup> or azides<sup>18</sup> instead of methyl groups, but this approach introduces additional challenges, such as differences in enzyme activity, cross-reactivity with native SAM, and validation of native substrate scope.

Taking inspiration from ligand-directed affinity labeling chemistries developed by Hamachi et al.<sup>19–21</sup> that demonstrate that high-affinity ligands with cleavable linkers can be used to promote traceless labeling of their target proteins, we looked to reverse the paradigm and use synthetic receptors<sup>22–25</sup> to direct affinity labeling of histone peptides containing the PTM trimethyl lysine (Kme3) (the ligand). Herein we transform a synthetic receptor for Kme3 into a chemical probe capable of selective turn-on fluorescence labeling of histone peptides containing Kme3. In our labeling scheme, receptor binding to Kme3 places the electrophile in close proximity to a

Received: March 17, 2016

Published: July 7, 2016

nucleophilic lysine on the target peptide, facilitating covalent labeling (Figure 1). We also demonstrate the utility of this

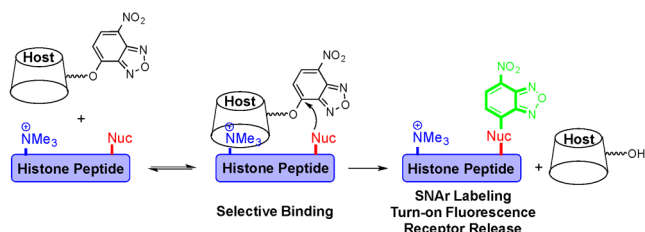


**Figure 1.** Turn-on fluorescence affinity labeling of a histone Kme3 peptide using a CX4-ONBD probe.

labeling strategy in the development of a turn-on fluorescence assay for screening inhibitors of histone deacetylase activity. This work represents the first example of synthetic-receptor directed affinity labeling and provides impetus for the use of synthetic receptors as agents for site-selective chemical modification of proteins mediated by PTMs.

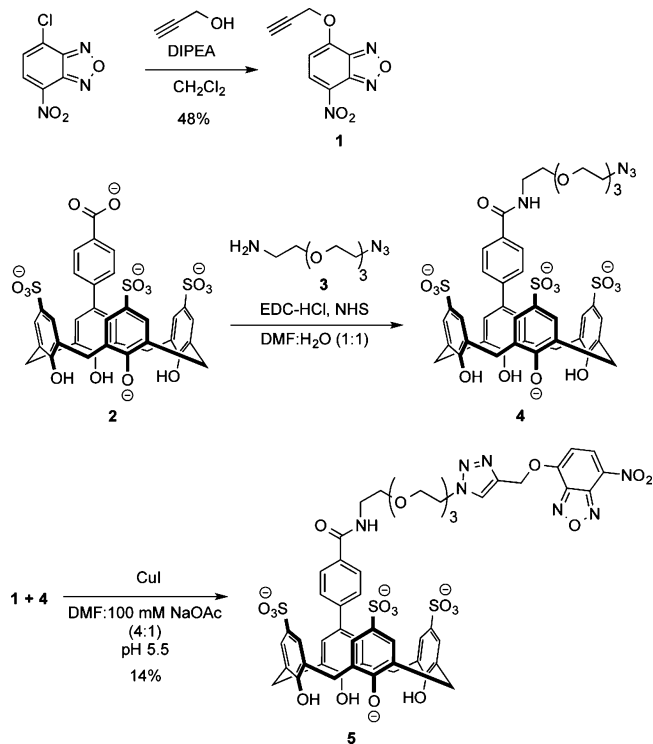
## RESULTS AND DISCUSSION

**Design and Synthesis of a Probe for Labeling for Kme3.** Analysis of histone sequences reveals that most known sites of Lys trimethylation contain another Lys 4–5 residues away, with a small number consisting of larger spacing between Kme3 and a neighboring Lys.<sup>26</sup> This pattern suggests that binding of a synthetic receptor to Kme3 brings it into close proximity of a nucleophilic residue, such that an affinity-labeling strategy is feasible. With the goal of preparing affinity probes capable of selective covalent labeling of histone peptides containing both Kme3 and a pendant unmethylated lysine, we designed a probe that features a synthetic receptor for Kme3 conjugated via a short flexible linker to a fluorogenic nitrobenzoxadiazole (NBD) group. For the synthetic receptor, we chose a trisulfonated calix-[4]-arene (CX4-Ar) receptor first reported by the Hof group<sup>24</sup> that shows preferential binding to trimethyl lysine over lower methylation states of lysine. An O-aryl NBD group was incorporated as a tag unit to allow for turn-on fluorescence labeling. In this labeling chemistry<sup>27</sup> developed by the Sodeoka lab, the ONBD unit serves as both an electrophilic site and a tag unit that selectively reacts with amines (i.e., lysine) with release of the receptor, leading to traceless fluorescent labeling of the target protein or peptide.

We prepared the CX4-ONBD probe **5** by assembling three separate components: propargyl ONBD compound **1**, CX4-Ar receptor **2**, and amino-azide linker **3** (Scheme 1). First, the alkyne functionalized NBD compound **1** was prepared by treating NBD chloride with propargyl alcohol in the presence of tertiary amine base. The synthetic receptor **2** was prepared with minor alterations to published procedure.<sup>24</sup> Likewise, the flexible amino-azide linker **3** was prepared according to previously reported procedure<sup>28</sup> starting from tetraethylene glycol. After preparing each of the three components, trisulfonated CX4-Ar receptor **2** was functionalized with linker **3** using carbodiimide coupling to produce azide-functionalized **4**. Finally, copper catalyzed azide–alkyne cycloaddition (CuAAC)<sup>29</sup> was used to conjugate alkyne **1** to azide **4**, generating the CX4-ONBD probe **5** which was purified by reversed-phase HPLC.

**Characterization of Binding by Isothermal Titration Calorimetry.** Previously reported binding studies<sup>24</sup> of **2**

## Scheme 1. Synthesis of CX4-ONBD Probe



indicate that the receptor has favorable binding to Kme3 in the context of a histone peptide. To determine whether covalent modification of this receptor influences binding, we measured the binding affinity of the CX4-ONBD probe **5** with a histone 3 (H3) peptide containing Kme3 (Table 1) using

**Table 1. Peptides Used for ITC, Fluorescence Labeling, and Deacetylase Activity Screening**

abbreviation	peptide sequence
K9me3R14	Ac-WGGGQTARK(me <sub>3</sub> )STGGGR-NH <sub>2</sub>
K9me3K14	Ac-WGGQTARK(me <sub>3</sub> )STGGK-NH <sub>2</sub>
K9K14	Ac-WGGQTARKSTGGK-NH <sub>2</sub>
K4me3K9ac	Ac-WGGTK(me <sub>3</sub> )QTARK(ac)STG-NH <sub>2</sub>
K4me3K9	Ac-WGGTK(me <sub>3</sub> )QTARKSTG-NH <sub>2</sub>
K27acK36me <sub>3</sub>	Ac-WGGRK(ac)SAPATGGVK(me <sub>3</sub> )-NH <sub>2</sub>
K27K36me <sub>3</sub>	Ac-WGGRKSAPATGGVK(me <sub>3</sub> )-NH <sub>2</sub>

isothermal titration calorimetry (ITC). Peptides were synthesized with an N-terminal WGG unit to facilitate calculation of peptide concentration by measuring absorbance at 280 nm. K9me3R14 was used in ITC experiments with **5**, where the lysine at position 14 was substituted for an arginine to prevent covalent labeling over the course of the ITC experiment without changing the overall charge of the peptide (Table 1). Under phosphate buffer conditions at pH 7.4 with no added salt (Table 2, entry 1), the CX4-ONBD probe had a  $K_d$  of 4.8  $\mu$ M for K9me3R14. While most examples of ligand-directed affinity labeling typically take advantage of ligands with submicromolar or nanomolar binding to their targets, it has been demonstrated that micromolar affinity interactions can provide an increase in effective molarity that is satisfactory for proximity-driven labeling.<sup>30</sup> Thus, we proceeded with evaluation of probe **5** as an affinity labeling probe.

**Table 2. Binding and Thermodynamic Data from ITC Experiments of 5 and 4 with K9me3K14 and K9K14**

entry	host	peptide	charge	$K_d$ ( $\mu\text{M}$ )	$\Delta G$ (kcal/mol)
1 <sup>a</sup>	5	K9me <sub>3</sub> R14	+3	4.8 ± 1.5	-7.3 ± 0.2
2 <sup>b</sup>	4	K9me <sub>3</sub> K14	+3	18.3 ± 7.7	-4.9 ± 0.6
3 <sup>b</sup>	4	K9K14	+3	>390	

<sup>a</sup>10 mM potassium phosphate, pH 7.4. <sup>b</sup>10 mM sodium borate, 100 mM NaCl, pH 8.6.

**Optimization of Receptor-Mediated Labeling.** To evaluate the degree of receptor-mediated labeling, probe 5 was incubated with either K9me3K14 or K9K14. It is important to note that both peptides have the same charge, so background electrostatic interactions are equivalent. However, K9K14 has two nucleophilic sites, versus only one for K9me3K14, which is expected to decrease the selectivity. Initially, concentrations well above the  $K_d$  were chosen for both probe and peptide to ensure complete host–guest complexation. Each peptide was incubated with probe 5 in 10 mM potassium phosphate buffer (pH 7.4) at room temperature for 24 h (Table 3), and the

**Table 3. Optimization of Labeling Reaction Conditions of CX<sub>4</sub>-ONBD Probe 5 with H3 Peptides**

peptide	conditions <sup>a,b</sup>	probe:peptide ( $\mu\text{M}$ )	labeling yield (%) <sup>c</sup>
K9K14	pH 7.4 <sup>a</sup>	100:100	12
K9me <sub>3</sub> K14	pH 7.4 <sup>a</sup>	100:100	29
K9K14	pH 8.6 <sup>b</sup>	100:50	70
K9me <sub>3</sub> K14	pH 8.6 <sup>b</sup>	100:50	75
K9K14	pH 8.6, 50 mM NaCl <sup>b</sup>	100:50	59
K9me <sub>3</sub> K14	pH 8.6, 50 mM NaCl <sup>b</sup>	100:50	82
K9K14	pH 8.6, 100 mM NaCl <sup>b</sup>	100:30	28
K9me <sub>3</sub> K14	pH 8.6, 100 mM NaCl <sup>b</sup>	100:30	68
K9K14	pH 8.6, 150 mM NaCl <sup>b</sup>	100:30	22
K9me <sub>3</sub> K14	pH 8.6, 150 mM NaCl <sup>b</sup>	100:30	65
K9K14	pH 8.6, 100 mM NaCl <sup>b</sup>	40:20	11
K9me <sub>3</sub> K14	pH 8.6, 100 mM NaCl <sup>b</sup>	40:20	61

<sup>a</sup>10 mM potassium phosphate, pH 7.4. <sup>b</sup>10 mM sodium borate, pH 8.6. <sup>c</sup>Yield is based on integration of the peaks in the HPLC trace; error is estimated at ±10% of the listed value for each entry.

labeling reactions were analyzed by HPLC (see Supporting Information). Reaction yields after 24 h revealed slow reactivity of the CX<sub>4</sub>-ONBD probe toward the representative histone peptides with modest 2:1 selective labeling for K9me3K14 over K9K14 (29% and 12% labeling yield, respectively). Since the O-aryl NBD group is known to be more reactive toward amine nucleophiles at higher pH,<sup>27</sup> the slow reactivity for our system could be attributed in part to the extent of protonation at pH 7.4 of the  $\epsilon$ -amino group of the lysine residues in the histone peptides. Expectedly, increasing the pH of the buffer used in the labeling reaction to 8.6 resulted in a marked rate acceleration. Unfortunately, this rate acceleration was accompanied by a complete loss in labeling selectivity for K9me3K14 over the K9K14 peptide (75% and 70% labeling yield, respectively).

To circumvent unselective labeling, we screened conditions with different concentrations of NaCl, as the concentration of salt in aqueous solutions is known to influence the strength of electrostatic interactions involved in host–guest complexation.<sup>31</sup> Varying NaCl concentration from 50 mM to 150 mM revealed two general trends: the overall labeling yield decreases slightly at higher concentrations of salt, while selectivity for K9me3K14 over K9K14 improves with increasing salt. Finally, we looked to improve selectivity further by lowering the concentration of both probe and peptide. Under conditions containing 40  $\mu\text{M}$  probe and 20  $\mu\text{M}$  peptide, the labeling selectivity improved to nearly 6-fold for K9me3K14 over K9K14. Also, despite micromolar binding and high salt concentration, the labeling rate for the reaction is appreciable even at lower concentrations of reagents, and the rate compares favorably to ligand-directed affinity labeling approaches.<sup>19,21,32</sup>

To determine the binding selectivity for Kme3 over unmethylated lysine under these optimized conditions, we used azide-functionalized receptor 4 as a surrogate for the CX<sub>4</sub>-ONBD probe as the azide is unreactive toward lysine-containing peptides during the ITC experiment. Additionally, 4 would not be expected to have binding interactions that are considerably different from 5 since the differences in functional groups between the two compounds are not close to the binding pocket. In 10 mM borate buffer with 100 mM NaCl (pH 8.6), receptor 4 exhibited about 20-fold selectivity for K9me3K14 over K9K14 with dissociation constants of 18.3  $\mu\text{M}$  and 390  $\mu\text{M}$ , respectively (Table 2, entries 2 and 3). This suggests that the affinity labeling is not achieving the maximum selectivity possible. Several factors likely contribute to this, including the flexibility of the linker that reduces the degree of preorganization as well as the fact that the unmethylated peptide has twice the number of reactive lysines, which reduces the selectivity.

**Receptor-Mediated Turn-On Fluorescence Labeling of Kme3 Peptides.** Next, we explored the turn-on fluorescence labeling of histone peptides by 5 by monitoring the fluorescence emission at 520 nm (excitation at 485 nm). Using optimized conditions of 40  $\mu\text{M}$  probe 5 and 20  $\mu\text{M}$  peptide in 10 mM phosphate buffer (100 mM NaCl, pH 8.6), measurements were taken every hour, and reactions were allowed to proceed under ambient temperature for 24 h (Figure 2). A pronounced turn-on fluorescence response was observed

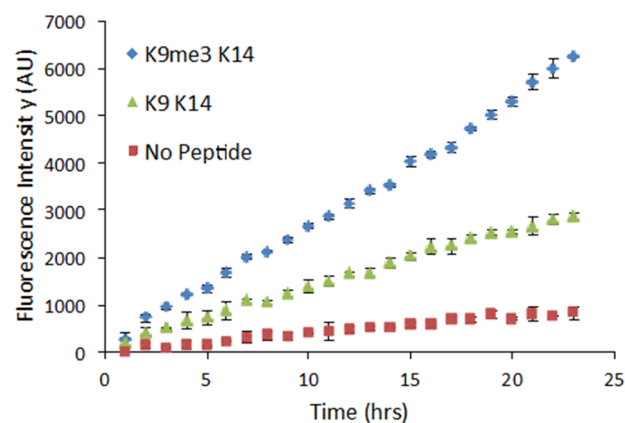


**Figure 2.** Turn-on fluorescence labeling of K9me3K14 and K9K14 peptides with Probe 5. Conditions: 40  $\mu\text{M}$  5 and 20  $\mu\text{M}$  peptide in 10 mM sodium borate buffer, pH 8.6, 100 mM NaCl.



for labeling of K9me3K14 with **5** (blue diamonds). On the other hand, the turn-on response for labeling with the K9K14 peptide (green triangles) was significantly lower, even though the peptide contains two reactive lysine residues. Trials with probe **5** alone appear to show only a slight increase in fluorescence signal over time, presumably due to slow hydrolysis of the O-NBD group.

Fluorescence labeling experiments were also performed with Propargyl ONBD **1** as a negative control to examine the contribution of the synthetic receptor to probe design and function. Under the same optimized reaction conditions employed for labeling with **5**, negative control **1** was allowed to react with K9K14 and with K9me3K14 for 24 h. Unlike probe **5**, labeling with the negative control was slow and nonselective (see [Supporting Information](#)). Moreover, compound **1** reacted with K9K14 to a greater extent than with K9me3K14 as the former contains two reactive lysine residues rather than just one. These results are consistent with HPLC analysis of labeling and further confirm that preferential binding of the receptor to Kme3 over K directly translates into favored turn-on fluorescence labeling of Kme3 histone peptides. To further confirm that the enhanced labeling rate of K9me3K14 by probe **5** is receptor mediated, a competition reaction was performed in which addition of K9me3R14, which can bind but not react with the probe, inhibited fluorescence labeling of K9me3K14 by probe **5** (see [Supporting Information](#)).

**Distance-Dependence of Labeling Rate.** To probe the distance-dependence of labeling, we also investigated the reaction of probe **5** with biologically relevant histone peptides with varying numbers of amino acids separating the Kme3 binding site and the pendant reactive amine ([Table 4](#)).

**Table 4. Peptides Used for Distance Dependence Labeling Experiments**

peptide	sequence	spacing
K36me3K37	Ac-WGGK(me <sub>3</sub> )KPHR-NH <sub>2</sub>	0
K4me <sub>3</sub> , N-term	H-ARTK(me <sub>3</sub> )GGW-NH <sub>2</sub>	2
K23K27me <sub>3</sub>	Ac-WGGKAARK(me <sub>3</sub> )-NH <sub>2</sub>	3
K4me <sub>3</sub> K9	Ac-WGGTK(me <sub>3</sub> )QTARKSTG-NH <sub>2</sub>	4
K27K36me <sub>3</sub>	Ac-WGGRKSAPATGGVK(me <sub>3</sub> )-NH <sub>2</sub>	8

Reactions were performed using 40  $\mu$ M **5** and 20  $\mu$ M peptide in 25 mM bicine buffer (137 mM NaCl, 2.7 mM KCl, 1 mM MgCl<sub>2</sub>, pH 8.02), and fluorescence measurements were taken after 24 h. Probe **5** reacted with K4me3K9 to the greatest extent, suggesting a preference for a spacing of four amino acids between Kme3 and the reactive amine ([Figure 3](#)). In contrast, K36me3K37 and K27K36me<sub>3</sub>, the two peptides with the shortest and longest spacing, respectively, showed considerably slower labeling. Interestingly, the peptide containing K4me3 and a free N-terminal amine (with a spacing of 2 amino acids) was the second most reactive in the series of peptides that were screened. This may be explained in part by the increased acidity of the alpha amino group relative to the  $\epsilon$  amine of the lysine side chain, making it a better nucleophile at pH 8. Unexpectedly, probe **5** reacted with K23K27me<sub>3</sub> (three amino acid spacing) the slowest, indicating that there may be subtleties in sequence and binding conformation that affect labeling rate in addition to amino acid spacing. While these results show some dependence of the rate of reaction on distance, all sequences tested gave a turn-on fluorescence

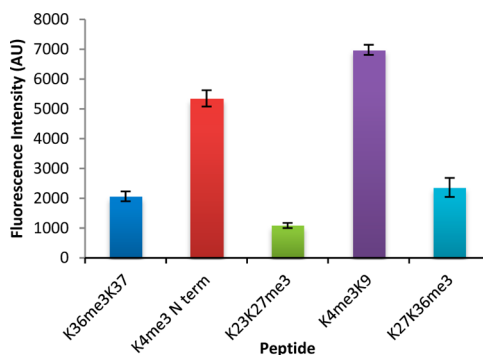


**Figure 3.** Analysis of distance dependence in the labeling of histone peptides by probe **5**. Fluorescence intensity is relative to probe **5** alone. Conditions: 40  $\mu$ M **5** and 20  $\mu$ M peptide in 25 mM bicine, 137 mM NaCl, 2.7 mM KCl, 1 mM MgCl<sub>2</sub>, pH 8.02, 24 h.

response which demonstrates the generality of **5** for labeling relevant histone H3 peptides.

**Receptor-Mediated Turn-On Fluorescence Assay for HDAC Activity.** After establishing selective turn-on fluorescence labeling of a Kme3 histone peptide, we applied this labeling methodology toward the development of a chemical assay for histone deacetylase (HDAC) activity. HDACs play a crucial role in regulating chromatin structure and ultimately gene expression via removal of acetyl groups from the side chains of acetylated lysine residues on histone tails.<sup>33,34</sup> Generally, deacetylation of histones is associated with a condensed chromatin state and repression of gene transcription. Many HDACs function as part of multiunit protein complexes and are implicated in processes ranging from cell differentiation to cell development.<sup>35,36</sup> Expectedly, dysregulation of HDACs often has detrimental biological effects, in some cases promoting oncogenesis or the development of inflammatory disease.<sup>37,38</sup>

Existing commercial kits for measuring HDAC activity predominantly rely on the use of a peptide or amino acid substrate with a C-terminal fluorogenic 7-amino-4-methylcoumarin tag directly linked to an acetylated lysine residue.<sup>39</sup> Removal of the acetyl group by an HDAC allows trypsin to be used in a subsequent development step to cleave the C-terminal amide, releasing a fluorophore. While this method is widely used and HDACs generally lack significant in vitro sequence selectivity, it is nonetheless severely limited in substrate scope since the coumarin tag must be immediately adjacent to the acetyl lysine. Furthermore, when screening for novel HDAC inhibitors, the required secondary trypsin reaction presents the possibility of false positives.<sup>40,41</sup> We envisioned designing a HDAC inhibitor assay in which probe **5** could be used to determine the extent of deacetylation in the context of a peptide containing an acetylated lysine residue nearby to trimethyl lysine. Trimethylation and acetylation of lysine are known to coexist and act cooperatively to influence the function of chromatin-modifying proteins.<sup>42</sup> Importantly, no background labeling is possible, as the substrate contains Kac and so has no nucleophilic site.

To demonstrate this assay concept, we utilized histone deacetylase 1 (HDAC1) as a model histone deacetylase. HDAC1 is a class I HDAC with a zinc dependent active site whose function is disrupted by inhibitors containing hydroxamate functionality, including vorinostat (SAHA).<sup>43</sup> For our assay, we prepared two H3 peptides representative of biologically relevant HDAC substrates (K4me3K9ac and

K27acK36me3). Histone H3 acetylation at K9 and K27 as well as methylation at K4 are histone PTMs known to be associated with active gene transcription.<sup>44,45</sup> Conversely, methylation at K36 has been linked to heterochromatin and may signal the recruitment of HDACs.<sup>46,47</sup> Furthermore, it has been shown that all four PTMs (K4me3, K9ac, K27ac, and K36me3) co-occur on a single H3 histone in cells treated with the HDAC inhibitor sodium butyrate.<sup>48</sup> These two peptides represent the extremes in optimal spacing, and so provide a good evaluation of applicability of an HDAC assay to both optimal and nonoptimal substrates.

Reactions between acetylated Kme3 peptides (200  $\mu$ M) and HDAC1 (0.1  $\mu$ g/ $\mu$ L) were carried out in 25 mM bicine buffer, 137 mM NaCl, 2.7 mM KCl, 1 mM MgCl<sub>2</sub> at pH 8.02 and 37 °C. After 1 h, reactions were diluted with the bicine reaction buffer to quench the reaction before addition to a 96-well plate containing 5. Fluorescence labeling was performed with a final concentration of 40  $\mu$ M 5 and 20  $\mu$ M peptide at ambient temperature for 24 h. Samples containing only 5 and HDAC1 were used as negative controls and showed a slow increase in fluorescence over time, likely due to the presence of the primary amine Tris in the stock buffer of the commercial enzyme (see Supporting Information). H3 peptides K4me3K9 and K27K36me3 were used as positive controls for determining the maximum extent of fluorescence labeling possible for peptides deacetylated by HDAC1. Additionally, the CX4-ONBD showed no reactivity toward the hydroxamate group of the SAHA inhibitor (see Supporting Information), which further displays the probe's selectivity toward amine nucleophiles.

Enzymatic assays with both the K4me3K9ac peptide and the K27acK36me3 peptide provide measurable turn-on fluorescence above background, and comparable fluorescence to the positive control (Figure 4). Indeed, the fact that the K27acK36me3 peptide achieves the full fluorescence intensity of the positive control, whereas the K4me3K9ac peptide does not regain full fluorescence suggests that K27acK36me3 is a more active substrate for HDAC1, which was confirmed by HPLC analysis (see Supporting Information). Thus, even though different spacing results in different maximum

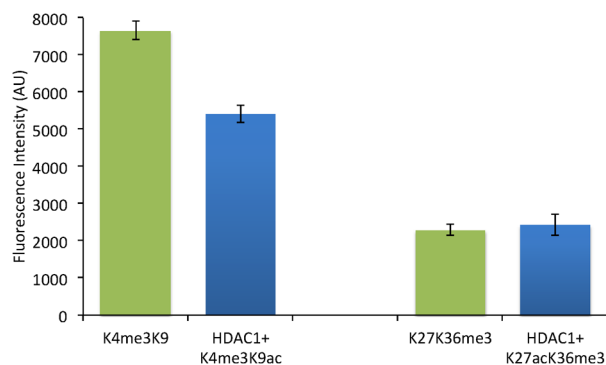


**Figure 4.** Turn-on fluorescence HDAC1 activity assay. Fluorescence monitoring of the deacetylation of histone H3 peptides K4me3 K9ac and K27ac K36me3 with probe 5 after reaction with HDAC1 for 1 h at 37 °C. Enzymatic conditions are described in the text. Fluorescence response is shown after labeling for 24 h. The fluorescence intensity for each reaction was normalized to the reaction containing HDAC1 and 5. Green bars: unacetylated control peptides K4me3K9 and K27K36me3; Blue bars: acetylated peptides K4me3K9ac or K27acK36me3 + HDAC1.

fluorescence at a given time point, the assay can still be used to measure substrate reactivity relative to positive controls. Moreover, analysis of the fluorescence output after 6 h exhibits identical results as the data at 24 h, despite low conversion, indicating that shorter assay times are feasible (see Supporting Information).

**Inhibition Assays and IC<sub>50</sub> Determination with Receptor-Mediated Turn-On Fluorescence Assay.** We next evaluated the ability to measure enzyme inhibition with probe 5, using two different HDACs, HDAC1 and HDAC3/NCOR1 (Figure 5). Enzymatic reactions with K4me3K9ac

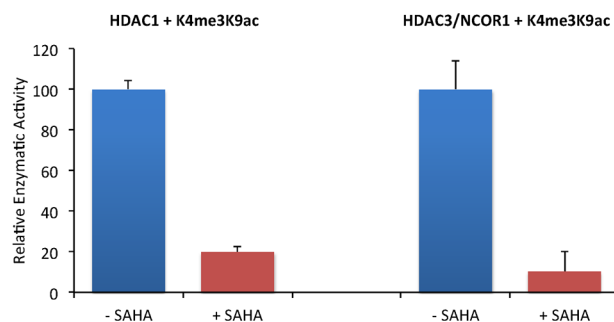


**Figure 5.** Inhibition assay. Fluorescence monitoring of the deacetylation of histone H3 peptide K4me3K9ac with probe 5 after reaction with HDAC1 or HDAC3/NCOR1 in the absence or presence of SAHA. Enzymatic conditions are described in the SI. Fluorescence response is shown after labeling for 24 h. The enzyme activity in the absence of SAHA was set to 100%. Blue bars: K4me3K9ac + HDAC; Red bars: K4me3K9ac + HDAC1 + SAHA.

were run in the absence or presence of SAHA. As can be seen in Figure 5, in both cases, a significant difference in turn-on fluorescence was observed, indicating that this probe can be used to qualitatively observe enzyme inhibition, and that the assay can be used for multiple HDACs.

To further validate the utility of our turn-on fluorescence assay for HDAC inhibitor screening, we carried out a dose–response experiment for the inhibition of HDAC3/NCOR1 by SAHA (Figure 6). For these experiments, inhibitor was serially diluted into 50 mM bicine buffer (137 mM NaCl, 2.7 mM KCl, 1 mM MgCl<sub>2</sub>, 0.5 mg/mL BSA, pH 8.0), and 11.2 nM HDAC3/NCOR1 was allowed to react with 100  $\mu$ M K4me3K9ac for 4 h at 37 °C. After quenching each reaction by the addition of 10  $\mu$ M SAHA, samples were added to a 96 well plate containing probe 5, giving a final concentration of 40  $\mu$ M 5, 75  $\mu$ M peptide, and 8.4 nM HDAC3/NCOR1. Fluorescence measurements were made after 24 h and were used to generate a dose–response curve. An IC<sub>50</sub> value of 1.3  $\pm$  0.3  $\mu$ M was determined for the inhibition of HDAC3/NCOR1 by SAHA, which is in close agreement with a previously reported measurement for inhibition of the decrotonylase activity of HDAC3/NCOR1 by SAHA using a 7-amino-4-methylcoumarin tagged substrate.<sup>49</sup> Overall these results demonstrate that probe 5 is able to efficiently detect deacetylase activity via a sensitive fluorogenic response and allows for accurate determination of IC<sub>50</sub> values, making it amenable to HDAC inhibitor screening.

## CONCLUSIONS

Herein we have described the development of a synthetic receptor probe for affinity labeling of Kme3-containing histone peptides, providing a turn-on fluorescence signal for the

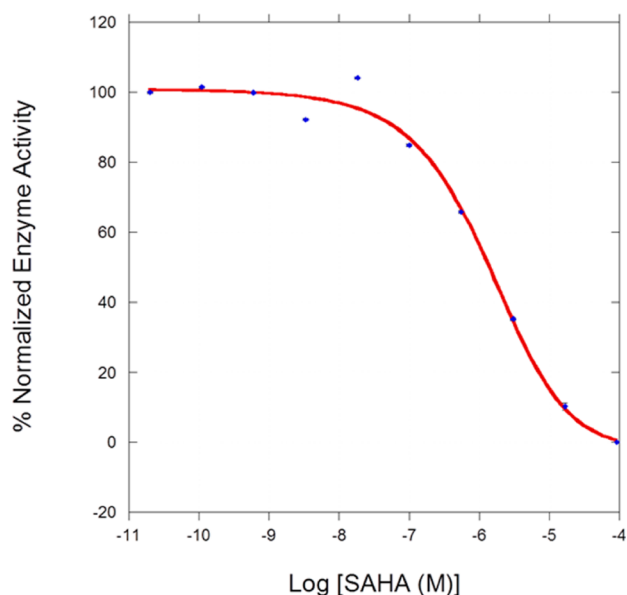


**Figure 6.** Dose–response curve of the inhibition of the HDAC3/NCOR1 catalyzed deacetylation of K4me3K9ac by SAHA. Data are an average of duplicate measurements. Conditions: 40  $\mu$ M 5, 75  $\mu$ M peptide, serial dilution of SAHA (starting from 92  $\mu$ M) in 50 mM bicine, 137 mM NaCl, 2.7 mM KCl, 1 mM MgCl<sub>2</sub>, pH 8.02, 24 h.

presence of Kme3. While ligand-directed affinity labeling is well established, this supramolecular approach reverses the paradigm, such that the receptor is the synthetic component and the ligand is the component to be labeled. To our knowledge, this is the first example of a labeling method using a synthetic receptor as an affinity labeling probe. We found that the rate and selectivity of the labeling reaction was considerably dependent on buffer pH, salt concentration, and reagent concentration. Using reaction buffer with slightly alkaline pH accelerated the labeling rate, while utilizing high salt concentration improved selectivity by minimizing nonspecific electrostatic interactions between the probe and peptide. Labeling was further improved by selecting concentrations that maintained appreciable host–guest complexation while exploiting the weaker binding of the unmethylated histone peptide at lower concentrations. Optimized labeling conditions lead to selective covalent modification and turn-on fluorescence in the reaction of the probe with the target peptide.

We illustrated the utility of this labeling approach in the development of a turn-on fluorescence HDAC assay. Inhibition of HDAC1 and HDAC3/NCOR1 activity by a known inhibitor, SAHA, could be monitored without the need for chromatographic separation of reaction components or a secondary trypsin development step. We also demonstrated the ability to determine IC<sub>50</sub>s using this probe. This HDAC assay has several advantages over the most commonly used HDAC assays, including a wider substrate scope and the lack of a secondary enzymatic step, and it is amenable to high-throughput screens in a plate-reader format. Finally, while the assay was demonstrated for monitoring deacetylase activity, this probe could theoretically be applied to other histone modifying enzymes such as acetyltransferases, demethylases, or methyltransferases.

## EXPERIMENTAL PROCEDURES

**Synthesis of 1.** 4-Chloro-nitrobenzo[c][1,2,5]oxadiazole (0.100 g, 0.50 mmol, 1 equiv) was dissolved in 5 mL CH<sub>2</sub>Cl<sub>2</sub> under a nitrogen

atmosphere. To this solution was added a mixture of propargyl alcohol (0.029 mL, 0.50 mmol, 1 equiv) and DIPEA (0.087 mL, 0.50 mmol, 1 equiv) in 5 mL CH<sub>2</sub>Cl<sub>2</sub>, and stirring was continued for 72 h. The solvent was removed under reduced pressure, and the crude product was purified by column chromatography (EtOAc/Hexanes 1:1) to give the product as a yellow-brown solid (0.053 g, 48%). <sup>1</sup>H NMR (CDCl<sub>3</sub>, 400 MHz): 8.558 (d, 1H, CH), 6.880 (d, 1H, CH), 5.129 (d, 2H, CH<sub>2</sub>), 2.720 (t, 1H, CH). MS (calculated): 242.02 [M + Na<sup>+</sup>]. HRMS (observed, ESI<sup>+</sup>): 242.01701 [M + Na<sup>+</sup>].

**Synthesis of 2.** Compound 2 was synthesized according to published procedure<sup>24</sup> on a 0.5 g scale but with a modified purification procedure. After completion of the reaction, solvent was removed under reduced pressure. The residue was taken up in MeOH/H<sub>2</sub>O (1:1), and Palladium was removed by QuadraPure TU resin. The resin (0.5 g) was added to the solution and heated to reflux under nitrogen for 24 h. The mixture was filtered, and the solvent was removed under reduced pressure. The crude product was used without further purification.

**Synthesis of 3.** Compound 3 was prepared according to published procedure.<sup>28</sup>

**Synthesis of 4.** EDC-HCl (0.087 g, 0.45 mmol, 2 equiv) and N-hydroxysuccinimide (0.050 g, 0.43 mmol, 2 equiv) were added to a solution of 2 (0.176 g, 0.22 mmol, 1 equiv) in 5 mL DMF/H<sub>2</sub>O (1:1) under a nitrogen atmosphere, and the mixture was stirred for 1 h. 3 (0.100 g, 0.46 mmol, 2.1 equiv) was added, and the solution was allowed to stir at room temperature overnight. The solvent was removed under reduced pressure, and the resulting residue was used in the next step without further purification. <sup>1</sup>H NMR (D<sub>2</sub>O, 600 MHz): 7.718 (d, 2H), 7.660 (d, 2H), 7.587 (d, 2H), 7.498 (d, 2H), 7.478 (s, 2H), 7.464 (s, 2H), 4.280 (d, 2H), 3.509–3.633 (m, 12H), 3.321 (s, 2H), 3.052 (s, 2H), 2.765 (s, 2H), 2.263 (s, 2H), 1.787 (t, 2H). MS (calculated): 983.18 [M – H], 1005.16 [M – 2H + Na<sup>+</sup>], 491.09 [M – 2H], 502.58 [M – 3H + Na<sup>+</sup>]. HRMS (observed, ESI<sup>-</sup>) 983.17713 [M – H], 1005.15929 [M – 2H + Na<sup>+</sup>], 491.08576 [M – 2H], 502.57840 [M – 3H + Na<sup>+</sup>].

**Synthesis of 5.** The crude residue containing 4 (0.037 g, 0.038 mmol, 1 equiv) and 1 (0.049 g, 0.22 mmol, 5.8 equiv) were dissolved in 5 mL DMF/100 mM sodium acetate, pH 5.5 (4:1). Copper iodide (0.001 g, 0.005 mmol, 0.13 equiv) was added, and the solution was allowed to stir at room temperature for 48 h. The solvent was removed under reduced pressure, and the resulting residue was purified by semipreparative reversed-phase HPLC (solvent A: 10 mM NH<sub>4</sub>OAc in 9:1 H<sub>2</sub>O:CH<sub>3</sub>CN; solvent B: 10 mM NH<sub>4</sub>OAc in 9:1 CH<sub>3</sub>CN:H<sub>2</sub>O) using the gradient: 0–100% B from 0 to 60 min with a flow rate of 4.0 mL/min to produce the desired compound in 14% yield. <sup>1</sup>H NMR (D<sub>2</sub>O, 600 MHz): 7.996 (s, 1H), 7.662 (s, 2H), 7.639 (s, 2H), 7.264–7.295 (m, 4H), 7.104–7.128 (m, 5H), 6.630 (d, 1H), 5.167 (s, 2H), 4.502 (t, 2H), 3.841 (t, 2H), 3.506–3.657 (m, 12H), MS (calculated) 1202.21 [M – H], 1224.18 [M – 2H + Na<sup>+</sup>], 600.60 [M – 2H], 611.59 [M – 3H + Na<sup>+</sup>]. HRMS (observed, ESI<sup>-</sup>) 1202.20580 [M – H], 1224.18764 [M – 2H + Na<sup>+</sup>], 600.59975 [M – 2H], 611.59092 [M – 3H + Na<sup>+</sup>].

Peptides were synthesized on a 0.6 mmol scale via solid-phase peptide synthesis in a peptide synthesis flask using Fmoc protected amino acids. Coupling reagents were HOBt/HBTU in DMF (4 equiv each), with coupling times of 60 min, followed by rinsing with DMF, MeOH, and CH<sub>2</sub>Cl<sub>2</sub>. Deprotection was performed with 20% piperidine in DMF. All peptides were acylated at the N-terminus with a solution of 5% acetic anhydride and 6% 2,6-lutidine in DMF. Cleavage was performed using a cocktail of 95% TFA/2.5% triisopropylsilane/2.5% H<sub>2</sub>O for 3 h. Peptides were purified by semipreparative reverse-phase HPLC on a C18 column at a flow rate of 4 mL/min. Peptides were purified with a linear gradient of A and B (A: 95% H<sub>2</sub>O/5% CH<sub>3</sub>CN with 0.1% TFA, B: 95% CH<sub>3</sub>CN/5% H<sub>2</sub>O with 0.1% TFA).

Methylated peptides were synthesized with 2 equiv of Fmoc-Lys(Me)<sub>2</sub>-OH HCl purchased from EMP Millipore and coupled for 5 h. The trimethyllysine containing peptides were synthesized by reacting corresponding dimethylated peptides (0.06 mmol scale) prior to cleavage from the resin with MTBD (7-Methyl-1,5,7-



triazabicyclo[4.4.0]dec-5-ene, 10 equiv) and methyl iodide (10 equiv) in DMF (5 mL) for 5 h with bubbling nitrogen in a peptide flask. After washing the resin with DMF and  $\text{CH}_2\text{Cl}_2$  and drying, the peptide was cleaved as normal.

Acetylated peptides were prepared from 4 equiv of Fmoc-Lys(ivDde)-OH purchased from Chem Impex with 1 h couplings. The ivDde group was deprotected using 5% hydrazine hydrate in DMF ( $3 \times 10$  mL) for 5 min. After washing resin with DMF, MeOH, and  $\text{CH}_2\text{Cl}_2$ , peptides were acetylated using a solution of 5% acetic anhydride and 6% 2,6-lutidine in DMF. Peptides were cleaved from the resin as normal after washing with DMF, MeOH, and  $\text{CH}_2\text{Cl}_2$ .

**Isothermal Titration Calorimetry.** ITC binding experiments were conducted using a Microcal AutoITC200. Titrations were performed at 25 °C in 10 mM potassium phosphate, pH 7.4 or 10 mM sodium borate, 100 mM NaCl, pH 8.6. The concentration of **5** was determined by measuring the UV-vis absorbance at 373 nm, using a NanoDrop2000 with a xenon flash lamp, 2048 element linear silicon CCD array detector, and 1 mm path length. The concentration of **4** was determined from UV-vis absorbance at 315 nm. Solutions of 0.9–1.2 mM of peptide were titrated into a 81–85  $\mu\text{M}$  solution of **4** or **5**, using 2.0  $\mu\text{L}$  increments every 3 min. Heats of dilution were subtracted prior to fitting. Binding curves were produced using the supplied Origin software and fit using one-site binding models.

**Fluorescence Labeling.** Fluorescence labeling experiments were performed in black 96 well optical bottom plates (nontreated, nonsterile, polystyrene) using a POLARstar Omega (BMG Labtech, Inc.) plate reader. A fluorescence optic with a 485 nm excitation filter and a 520 nm emission filter was used. Labeling reactions were carried out at ambient temperature, and Titer Tops sealing film was used to prevent evaporation. Fluorescence intensity was measured every hour for 24 h.

**In Vitro HDAC Assay.** Enzymatic reactions with HDAC1 were performed at 37 °C in 25 mM bicine buffer, 137 mM NaCl, 2.7 mM KCl, 1 mM  $\text{MgCl}_2$ , pH 8.02, with 0.1  $\mu\text{g}/\mu\text{L}$  HDAC1 and 200  $\mu\text{M}$  acetylated peptide. After 1 h, the reactions were diluted with buffer before adding to a 96-well plate containing probe **5** to give final concentrations of 20  $\mu\text{M}$  peptide, 40  $\mu\text{M}$  probe **5**, and 10 ng/ $\mu\text{L}$  HDAC1 (reactions containing SAHA were diluted to contain 5  $\mu\text{M}$  SAHA). Fluorescence labeling was monitored every hour for 24 h.

For in vitro inhibition experiments with HDAC3/NCOR1, a 5.5 dilution series (starting with 92  $\mu\text{M}$  SAHA) was prepared in 50 mM bicine buffer, 137 mM NaCl, 2.7 mM KCl, 1 mM  $\text{MgCl}_2$ , 0.5 mg/mL BSA (pH 8.02). Enzymatic reactions were performed using 11.2 nM HDAC3/NCOR1 (purchased from Enzo Life Sciences) and 100  $\mu\text{M}$  acetylated peptide at 37 °C. After 4 h, the reactions were quenched with 10  $\mu\text{M}$  SAHA before adding to a 96-well plate containing probe **5** to give final concentrations of 77  $\mu\text{M}$  peptide, 40  $\mu\text{M}$  probe **5**, and 8.6 nM HDAC3/NCOR1. Fluorescence labeling was monitored after 24 h.

## ■ ASSOCIATED CONTENT

### ● Supporting Information

The Supporting Information is available free of charge on the ACS Publications website at DOI: 10.1021/jacs.6b02836.

Synthesis of compounds, NMR and mass spectrometric characterization, ITC binding data, LCMS and HPLC analysis of labeling, affinity labeling control experiments, turn-on fluorescence HDAC assay data, and experimental procedures. (PDF)

## ■ AUTHOR INFORMATION

### Corresponding Author

\*mlwaters@email.unc.edu

### Notes

The authors declare no competing financial interest.

## ■ ACKNOWLEDGMENTS

Funding for this work was provided in part by the W. M. Keck Foundation. This material is based upon work supported in part by the National Science Foundation under Grant No. CHE-1306977.

## ■ REFERENCES

- (1) Sidoli, S.; Cheng, L.; Jensen, O. N. *J. Proteomics* **2012**, *75*, 3419–3433.
- (2) Carlson, S. M.; Gozani, O. *J. Mol. Biol.* **2014**, *426*, 3350–3362.
- (3) Jones, P. A.; Baylin, S. B. *Cell* **2007**, *128*, 683–692.
- (4) Blow, N. *Nature* **2007**, *447*, 741–744.
- (5) Kazanekci, C. C.; Kowalski, A. J.; Ding, T.; Rittling, S. R.; Denhardt, D. T. *J. Cell. Biochem.* **2007**, *102*, 925–935.
- (6) Rothbart, S. B.; Dickson, B. M.; Raab, J. R.; Grzybowski, A. T.; Krajewski, K.; Guo, A. H.; Shanle, E. K.; Josefovicz, S. Z.; Fuchs, S. M.; Allis, C. D.; Magnuson, T. R.; Ruthenburg, A. J.; Strahl, B. D. *Mol. Cell* **2015**, *59*, 502–511.
- (7) Carlson, S. M.; Moore, K. E.; Green, E. M.; Martin, G. M.; Gozani, O. *Nat. Protoc.* **2014**, *9*, 37–50.
- (8) Bremang, M.; Cuomo, A.; Agresta, A. M.; Stugiewicz, M.; Spadotto, V.; Bonaldi, T. *Mol. Biosyst.* **2013**, *9*, 2231–2247.
- (9) Guo, A.; Gu, H.; Zhou, J.; Mulhern, D.; Wang, Y.; Lee, K. A.; Yang, V.; Aguiar, M.; Kornhauser, J.; Jia, X.; Ren, J.; Beausoleil, S. A.; Silva, J. C.; Vemulapalli, V.; Bedford, M. T.; Comb, M. J. *Mol. Cell. Proteomics* **2014**, *13*, 372–387.
- (10) Geoghegan, V.; Guo, A.; Trudgian, D.; Thomas, B.; Acuto, O. *Nat. Commun.* **2015**, *6*, 6758.
- (11) Choudhary, C.; Kumar, C.; Gnad, F.; Nielsen, M. L.; Rehman, M.; Walther, T. C.; Olsen, J. V.; Mann, M. *Science* **2009**, *325*, 834–840.
- (12) Choudhary, C.; Weinert, B. T.; Nishida, Y.; Verdin, E.; Mann, M. *Nat. Rev. Mol. Cell Biol.* **2014**, *15*, 536–550.
- (13) Gronborg, M. *Mol. Cell. Proteomics* **2002**, *1*, 517–527.
- (14) Witze, E. S.; Old, W. M.; Resing, K. A.; Ahn, N. G. *Nat. Methods* **2007**, *4*, 798–806.
- (15) Bicker, K. L.; Subramanian, V.; Chumanevich, A. A.; Hofseth, L. J.; Thompson, P. R. *J. Am. Chem. Soc.* **2012**, *134*, 17015–17018.
- (16) Bothwell, I. R.; Islam, K.; Chen, Y.; Zheng, W.; Blum, G.; Deng, H.; Luo, M. *J. Am. Chem. Soc.* **2012**, *134*, 14905–14912.
- (17) Binda, O.; Boyce, M.; Rush, J. S.; Palaniappan, K. K.; Bertozzi, C. R.; Gozani, O. *ChemBioChem* **2011**, *12*, 330–334.
- (18) Islam, K.; Bothwell, I.; Chen, Y.; Sengelaub, C.; Wang, R.; Deng, H.; Luo, M. *J. Am. Chem. Soc.* **2012**, *134*, 5909–5915.
- (19) Tsukiji, S.; Miyagawa, M.; Takaoka, Y.; Tamura, T.; Hamachi, I. *Nat. Chem. Biol.* **2009**, *5*, 341–343.
- (20) Koshi, Y.; Nakata, E.; Miyagawa, M.; Tsukiji, S.; Ogawa, T.; Hamachi, I. *J. Am. Chem. Soc.* **2008**, *130*, 245–251.
- (21) Fujishima, S.; Yasui, R.; Miki, T.; Ojida, A.; Hamachi, I. *J. Am. Chem. Soc.* **2012**, *134*, 3961–3964.
- (22) Beshara, C. S.; Jones, C. E.; Daze, K. D.; Lilgert, B. J.; Hof, F. *ChemBioChem* **2010**, *11*, 63–66.
- (23) Ingerman, L. A.; Cuellar, M. E.; Waters, M. L. *Chem. Commun.* **2010**, *46*, 1839.
- (24) Daze, K. D.; Ma, M. C. F.; Pineux, F.; Hof, F. *Org. Lett.* **2012**, *14*, 1512–1515.
- (25) James, L. I.; Beaver, J. E.; Rice, N. W.; Waters, M. L. *J. Am. Chem. Soc.* **2013**, *135*, 6450–6455.
- (26) Ohe, Y.; Iwai, K. *J. Biochem.* **1981**, *90*, 1205–1211.
- (27) Yamaguchi, T.; Asanuma, M.; Nakanishi, S.; Saito, Y.; Okazaki, M.; Dodo, K.; Sodeoka, M. *Chem. Sci.* **2014**, *5*, 1021.
- (28) Bongers, R. M.; van den Berg, R. J. B. H. N.; Heitman, L. H.; IJzerman, A. P.; Oosterom, J.; Timmers, C. M.; Overkleeft, H. S.; van der Marel, G. A. *Bioorg. Med. Chem.* **2007**, *15*, 4841–4856.
- (29) Rostovtsev, V. V.; Green, L. G.; Fokin, V. V.; Sharpless, K. B. *Angew. Chem., Int. Ed.* **2002**, *41*, 2596–2599.
- (30) Huang, F.; Nie, Y.; Ye, F.; Zhang, M.; Xia, J. *Bioconjugate Chem.* **2015**, *26*, 1613.

- (31) Daze, K. D.; Jones, C. E.; Lilgert, B. J.; Beshara, C. S.; Hof, F. *Can. J. Chem.* **2013**, *91*, 1072–1076.
- (32) Takaoka, Y.; Nishikawa, Y.; Hashimoto, Y.; Sasaki, K.; Hamachi, I. *Chem. Sci.* **2015**, *6*, 3217–3224.
- (33) Cheung, W. L.; Briggs, S. D.; Allis, C. D. *Curr. Opin. Cell Biol.* **2000**, *12*, 326–333.
- (34) Strahl, B. D.; Allis, C. D. *Nature* **2000**, *403*, 41–45.
- (35) Lai, A. Y.; Wade, P. A. *Nat. Rev. Cancer* **2011**, *11*, 588–596.
- (36) Denslow, S. A.; Wade, P. A. *Oncogene* **2007**, *26*, 5433–5438.
- (37) Huang, L. J. *Cell. Physiol.* **2006**, *209*, 611–616.
- (38) Lin, H.-Y.; Chen, C.-S.; Lin, S.-P.; Weng, J.-R.; Chen, C.-S. *Med. Res. Rev.* **2006**, *26*, 397–413.
- (39) Hoffmann, K.; Jung, M.; Brosch, G.; Loidl, P. *Nucleic Acids Res.* **1999**, *27*, 2057–2058.
- (40) Acker, M. G.; Auld, D. S. *Perspect. Sci.* **2014**, *1*, 56–73.
- (41) Sodji, Q. H.; Kornacki, J. R.; Mrksich, M.; Oyelere, A. K. *Epigenetic Technological Applications*; Elsevier, 2015.
- (42) Schwämmle, V.; Aspalter, C.-M.; Sidoli, S.; Jensen, O. N. *Mol. Cell. Proteomics* **2014**, *13*, 1855–1865.
- (43) Marks, P. A.; Breslow, R. *Nat. Biotechnol.* **2007**, *25*, 84–90.
- (44) Martin, C.; Zhang, Y. *Nat. Rev. Mol. Cell Biol.* **2005**, *6*, 838–849.
- (45) Eberharter, A.; Becker, P. B. *EMBO Rep.* **2002**, *3*, 224–229.
- (46) Chantalat, S.; Depaux, A.; Héry, P.; Barral, S.; Thuret, J.-Y.; Dimitrov, S.; Gérard, M. *Genome Res.* **2011**, *21*, 1426–1437.
- (47) Carrozza, M. J.; Li, B.; Florens, L.; Suganuma, T.; Swanson, S. K.; Lee, K. K.; Shia, W.-J.; Anderson, S.; Yates, J.; Washburn, M. P.; Workman, J. L. *Cell* **2005**, *123*, 581–592.
- (48) Young, N. L.; DiMaggio, P. A.; Plazas-Mayorca, M. D.; Baliban, R. C.; Floudas, C. A.; Garcia, B. A. *Mol. Cell. Proteomics* **2009**, *8*, 2266–2284.
- (49) Madsen, A. S.; Olsen, C. A. *Angew. Chem., Int. Ed.* **2012**, *51*, 9083–9087.